A&A 368, 721–729 (2001)
DOI: 10.1051/0004-6361:20000576

Astronomy & Astrophysics

Laboratory investigation of crystallisation in annealed amorphous $MgSiO_3$

S. P. Thompson and C. C. Tang

Daresbury Laboratory, Synchrotron Radiation Department, Warrington, Cheshire WA4 4AD, UK

Received 11 October 2000 / Accepted 22 December 2000

Abstract. In situ high resolution synchrotron X-ray powder diffraction measurements are used to probe the structural changes in a sample of amorphous $MgSiO_3$ during annealing. Temperatures cover the astrophysically significant range 1000 K to 1173 K and prior to annealing the sample showed typical amorphous structure. Following ∼2 hours annealing at 1000 K an initial crystallite had formed that was coexistent with a modified amorphous component. Increases in temperature coupled with long annealing times produced no further change to the amorphous component and only very minor changes in the appearance of the crystalline phase. This we identify as a structural stall in the crystallisation process and is likely to be the origin of the spectral stall reported for similar silicate materials. Finally at 1173 K, following a cumulative annealing time of ∼79 hours, the amorphous background began to collapse coinciding with the development of further crystalline features. The stall in structural development arises because the crystallisation process is in part regulated by the amorphous phase during annealing. At low-end temperatures it is likely that the annealing process itself strengthens the amorphous phase allowing it to survive up to relatively high temperatures. This finding suggests that some lower temperature information may be preserved in certain cosmic dust grains that were initially annealed at lower temperatures.

Key words. methods: laboratory – comets: general – solar system: general – stars: circumstellar matter – stars: AGB and post-AGB

1. Introduction

The observed 10 μm band profiles attributable to silicate dust grains reflect the mineralogy and degree of crystallinity of those grains. Silicate grains in molecular clouds show broad, smooth features with a maximum near 9.7 μm typical of amorphous grains (Day 1974). In contrast, certain comets such as Halley (Bregman et al. 1987; Campins & Ryan 1989) and several new and long period comets, including Hale-Bopp (Crovisier et al. 1996; Russell & Lynch 1996; Hayward & Hanner 1997) show spectral peaks at 11.2 μm, more characteristic of crystalline olivine. Since it is generally assumed that comets form from essentially pristine unaltered interstellar material in the cold outer solar nebula, the presence of crystalline grains in comet dust but not molecular cloud dust is problematic.

Amorphous grains of olivine and pyroxene composition are widely accepted as ubiquitous constituents of circumstellar, interstellar and interplanetary dust. Their formation in O-rich circumstellar outflows is initiated by the nucleation of SiO, followed by the condensation of additional refractory components such as MgO. Conversion to amorphous silicate then occurs via solid phase reaction. The optical characterisation of amorphous silicates has previously been the subject of much laboratory work (e.g. Nuth & Donn 1982; Hecht et al. 1986; Dorschner et al. 1988; Stephens et al. 1995). However the existence of crystalline cometary features and more recently with the advent of ISO, the widespread detection of crystalline features in the spectra of certain classes of star (Waters et al. 1996; Tielens et al. 1998), shows that it has now become desirable to study the evolution of these materials at higher temperatures since the genetic relationship between the populations of crystalline and amorphous silicates in the various stellar and solar system environments is unclear. Indeed the common assumption that the ISO detected circumstellar olivine crystals are the result of the annealing of amorphous grains is by no means certain. Many of the ISO crystallites were identified from strong far–IR resonances associated with olivine, which have yet to be reproduced in the laboratory by annealing amorphous silicates (Hallenbeck et al. 1998; Wooden et al. 1999). There is thus a clear need for a fundamental laboratory investigation of the crystallisation process for silicates in order to place firmer constraints

Send offprint requests to: S. P. Thompson
e-mail: s.p.thompson@dl.ac.uk

on the possible conditions and processes to which cosmic grains are subjected.

Early laboratory work on the thermal processing of amorphous silicates (e.g. Koike & Tsuchiyama 1991; Koike & Tsuchiyama 1992; Thompson et al. 1996) found the temperature threshold for re-crystallisation to be in the region of 973 K, which placed clear upper limit constraints on the thermal history of amorphous grains. More recently this view has been refined by investigation of the spectral evolution of the 10 μm band in the laboratory as a function of both annealing temperature and annealing time (Hallenbeck & Nuth 1998; Hallenbeck et al. 1998, both papers referred to collectively hereafter as HN&D). To briefly summarise these results, at 1027 K and 6 hours annealing, the spectral maximum shifted from an initial 9.3 μm to 9.74 μm, which is characteristic of amorphous astronomical silicates (and indicates that all freshly nucleated grains in circumstellar outflows have undergone some degree of thermal processing). Following 10.5 hours at the same temperature dual maxima developed at 9.8 μm and 11 μm. After a subsequent total of 37.5 hours no further changes had developed. HN&D termed this a *spectral stall* and proposed it to be a natural pause in development midway between chaotic and ordered glassy structures, but did not investigate its physical mechanism empirically. Upon exiting the stall period, following further annealing, maxima at 9.1 μm, 9.8 μm and 11 μm were observed. HN&D identified the major crystallite as forsterite and obtained a good fit to their IR data using a mixture of forsterite and silica reference spectra. By studying entry time and duration of the stall as a function of temperature HN&D calculated that annealing at 1000 K would require 25 ± 3 days to reach the stall, which should then persist for around 300 days. At the other extreme, annealing at 1060 K should result in a sample passing through the stall state without pausing. HN&D concluded that the temperatures experienced by comets during their passage near the Sun are insufficient to produce olivine rich spectra. Furthermore, given that such features have been observed in the dynamically young comet Mueller (Hanner 1994), it is likely that crystallisation must have occurred prior to inclusion in the comet body.

In this paper we report on a laboratory study into the structural development of crystallinity in amorphous $MgSiO_3$ using synchrotron X-ray powder diffraction data collected during the annealing process. Due to limitations in data collection times for wide angle scans ($\sim$1.6 hours per scan), we could not study the evolution as a function of annealing time in fine detail and defer the results of a higher time-resolved study to a later paper. We have however identified the occurrence of a structural stall during the development of crystallinity that is likely to be the physical origin of the spectral stall reported by HN&D. We also find that during this stall period a significant amorphous component persists up to high temperatures and discuss evidence suggesting that the thermal survivability of this phase is enhanced by initial exposure to lower ($\sim$1000 K) temperatures.

2. Experimental details

Based on the parallel beam optics of Parrish et al. (1986), the Daresbury synchrotron radiation source station 2.3 diffractometer used in our experiment was originally constructed for ambient high-resolution powder diffraction studies (Cernik et al. 1990; Collins et al. 1992). Located 15 m tangentially from a 1.2 T dipole magnet in the 2 GeV electron storage ring (Munro 1997) it receives X-rays in the range 0.7–2.5 Å. These are filtered by a water cooled Si(III) channel-cut single crystal to give a monochromatic beam incident at the centre of the two circle (θ and 2θ) diffractometer. The furnace is mounted on the θ-circle with a flat-plate sample holder inside the device at the centre of the θ-circle so that Hart-Parrish diffraction geometry is achieved (Hart & Parrish 1986). This makes the diffraction optics insensitive to changes in sample height, which is essential as small movements are inevitable when the sample is heated. The diffracted beam passes through a parallel foil assembly on the 2θ arm and is detected using an enhanced dynamic range scintillation counter.

The furnace itself is based on a design by Debrenne et al. (1970), details of which are given in Tang et al. (1998). The sample crucible is made of molybdenum, chosen for its high melting point and induction characteristics, while a 1 mm deep and 15 mm diameter pressed platinum former is placed on the crucible to hold the sample and to prevent possible chemical reaction between sample and crucible at high temperatures. Heating is via a water-cooled 2 kW RF copper coil regulated by a Eurotherm 900 controller. Sample temperature is measured by a tungsten-rhenium thermocouple placed at the sample/crucible assembly. The operational temperature range is 290–2000 K with a heating response time of $\sim$30 s. Even at high temperatures, $\pm$1 K stability is achieved in under a few minutes. The whole furnace assembly is enclosed in a stainless steel body, with incident and diffracted X-rays passing through kapton entrance and exit windows allowing measurements to be made during annealing.

Normally θ–2θ diffraction patterns are collected by synchronised rotation of the θ and 2θ arms. However to prevent the sample falling from the holder at high angle, the θ circle was fixed so that the sample was inclined at 10° to the horizontal incoming beam and the diffraction intensities corrected accordingly. An X-ray wavelength of 1.2995 Å was selected as a good compromise between peak incident flux and the requirement for low wavelength for increased X-ray wave vector k-space sampling within the silicate sample. Scan parameters of a 2θ step size of 10mdeg and detector integration time of 1 s per point were used throughout. In order to ramp our sample up to the initial temperature of 1000 K used as the starting point in our experiment, the temperature was increased in steps of $\sim$200 K over a period of approximately 5 min,

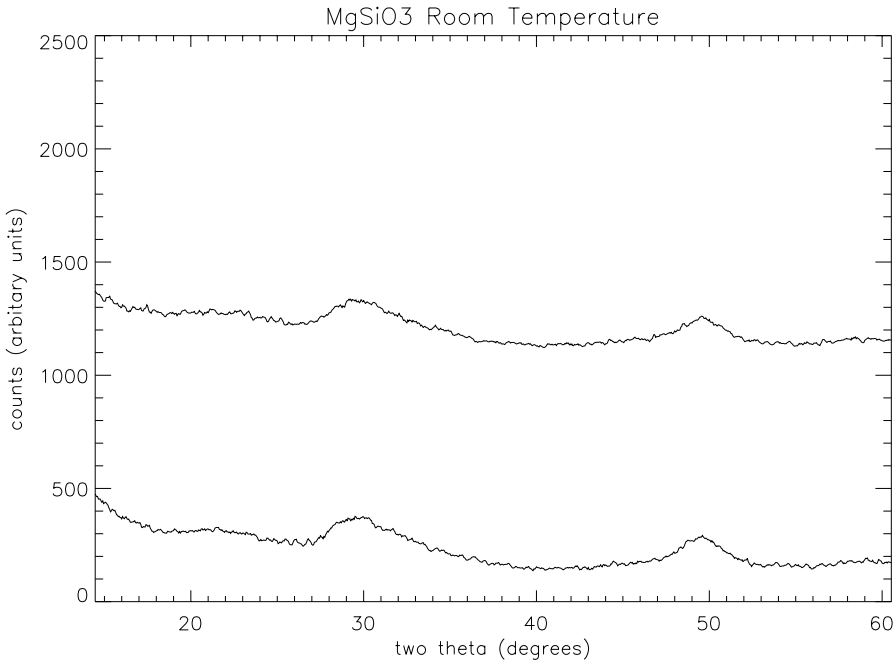

Fig. 1. X-ray powder diffraction patterns for amorphous $MgSiO_3$ recorded at room temperature. Patterns in this and subsequent figures have been offset in the y-axis direction for clarity

with the approach to 1000 K being made in progressively smaller increments to avoid overshoot of the target temperature. Data collection began as soon as the temperature stabilised at 1000 K (approximately 2 min).

Our sample was produced using the gel desiccation method (Sabatier 1950; Day 1974) according to the following recipe:

1. 0.1 M solutions of the soluble metal salts $MgCl_2$ and Na_2SiO_3 (sodium metasilicate) were mixed in the correct stoichiometric ratio to produce $MgSiO_3$;
2. The white suspension thus formed was left to settle for two days. The excess liquid was then decanted off and the remaining suspension centrifuged and washed with distilled water. This centrifuging/washing cycle was repeated three times;
3. The resulting gelatinous precipitate was then dried in air over a hot plate (100–150 °C) to yield lumps of a white glassy-looking solid;
4. To prepare the sample for presentation to the synchrotron beam it was then ground by hand in a pestle and mortar to give a fine-grained powder. The largest grains were typically ∼0.1 mm in diameter.

3. Results

Initially the sample was scanned at room temperature (Fig. 1), before raising its temperature to 1000 K. The sample was then held constant at this temperature and repeatedly scanned automatically for 19.5 hours. During this time the diffraction patterns showed the evolution of a crystallite (Fig. 2). At the end of this period a developed crystalline diffraction pattern was visible in the data, superposed upon an amorphous background that had changed little throughout annealing. The crystalline component had begun to form after only ∼2 hours and after ∼5 hours annealing had developed to its full extent with both crystalline and amorphous components changing little from then on. The temperature was then increased to 1031 K and the sample annealed for a further 24.5 hours (Fig. 3). During this period no major changes in either amorphous or crystalline patterns occurred, except for the sharpening of a few very weak crystalline peaks. Further processing for 24 hours at the increased temperature of 1043 K again produced no major change (Fig. 4). Following this the sample temperature was raised in steps through 1083 K, 1113 K and 1143 K with a further total annealing time of 5 hours (Fig. 5). Again, no change to either component was observed. Finally raising the temperature to 1173 K, the sample was processed for a further 14.5 hours. It was during this time that the sample structure changed. After 5-6 hours at this temperature, the sample underwent rapid modification (Fig. 6), evidenced by changes in width and profile of the amorphous features, sharpening and growth of existing crystalline peaks and development of new diffraction features.

Table 1 compares strongest peak positions and d-spacings (the distances between successive ordered planes of reflecting atoms) for the 1000 K and 1173 K crystallites to reference data from the *International Committee for Powder Diffraction Standards* (ICPDS) database. In both, the crystalline structure is accounted for by forsterite. However, at 1173 K a small number of peaks remain unidentified and may possibly indicate the presence of a second minor crystalline phase. None of the unidentified features however correspond to crystalline SiO_2. It is also

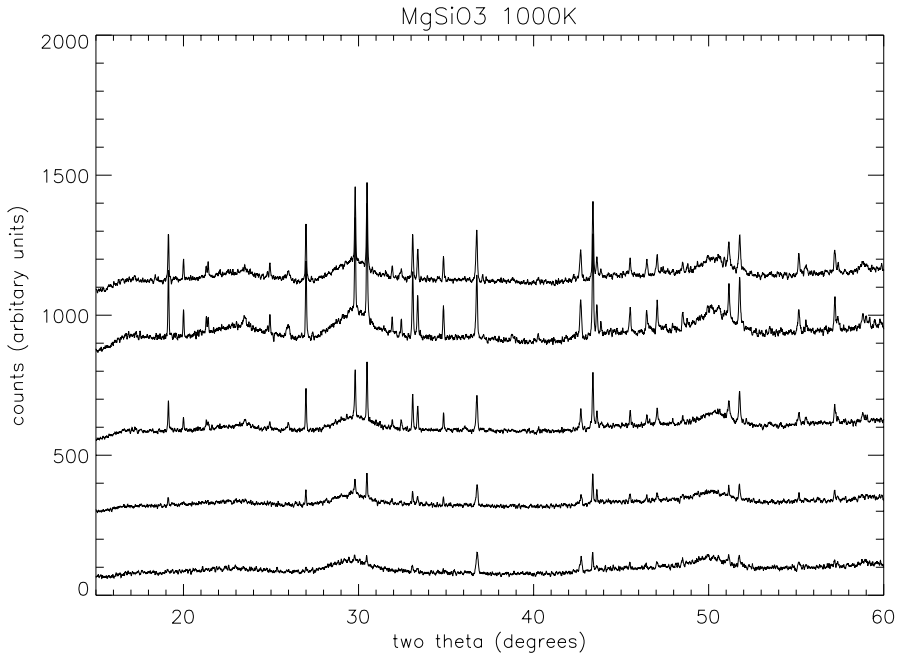

Fig. 2. Diffraction patterns for $MgSiO_3$ sample recorded at 1000 K: bottom pattern is initial exposure, top pattern after 19.5 hours annealing, middle patterns are sample data for intermediate annealing times

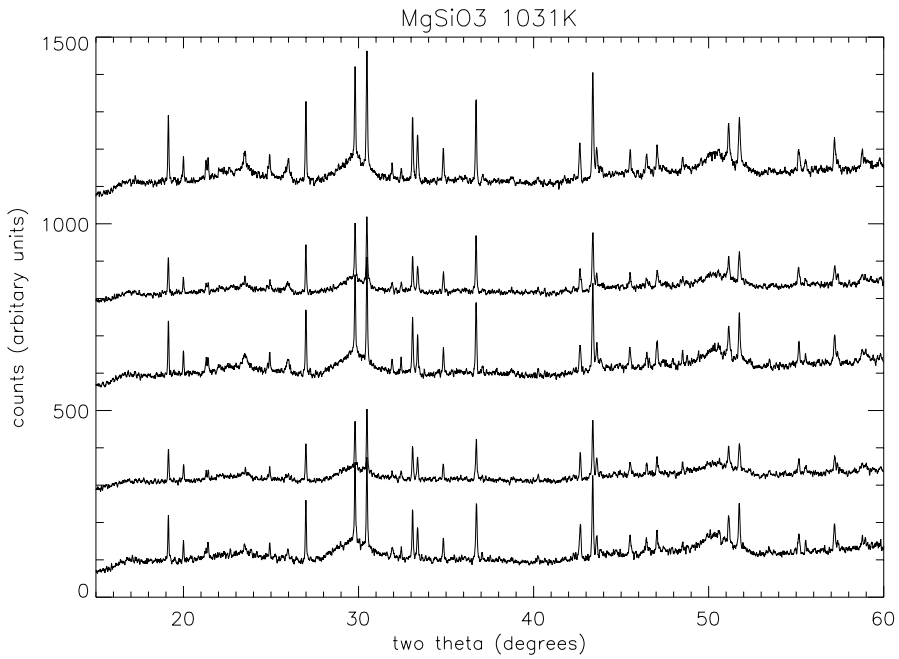

Fig. 3. $MgSiO_3$ diffraction patterns recorded at 1031 K: bottom pattern is initial exposure at this temperature, top pattern after 24.5 hours, middle patterns are sample data for intermediate times. Note the correspondence between these patterns and the top two patterns of Fig. 2

worth remarking that the open olivine Mg_2SiO_4 forsterite structure would seem to be compositionally unfavourable for a sample of $MgSiO_3$. Although crystalline $MgSiO_3$ (e.g. enstatite) can be expected to yield some diffraction peaks coincident or close to those of forsterite, forsterite accounts for all the lower temperature crystal structure and nearly all the higher temperature crystal structure in our data.

The persistence of the amorphous component throughout the annealing process is illustrated by the widths of the two broad features centred at $\sim 30^\circ$ and $\sim 50^\circ$ 2θ. Prior to annealing these widths were $\sim 8.5^\circ$ and $\sim 6^\circ$ 2θ respectively, while after initial annealing at 1000 K they had shrunk to $\sim 4^\circ$ each and remained essentially constant throughout the remainder of the experiment until

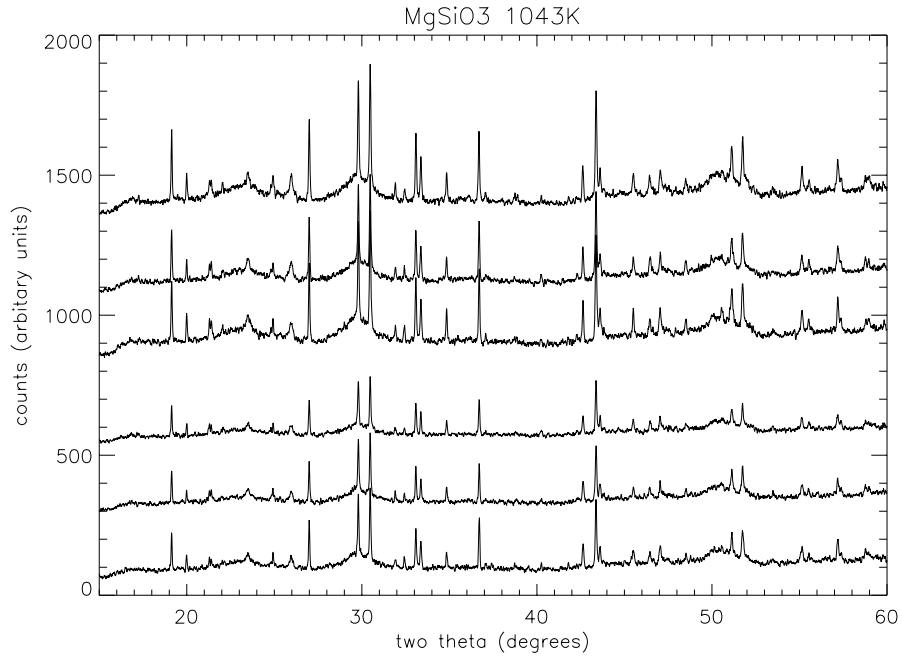

Fig. 4. $MgSiO_3$ diffraction patterns recorded at 1043 K: bottom pattern is initial exposure, top pattern after 24 hours, middle patterns are sample data for intermediate times. Note the overall correspondence to the lower temperature structure shown in Fig. 3

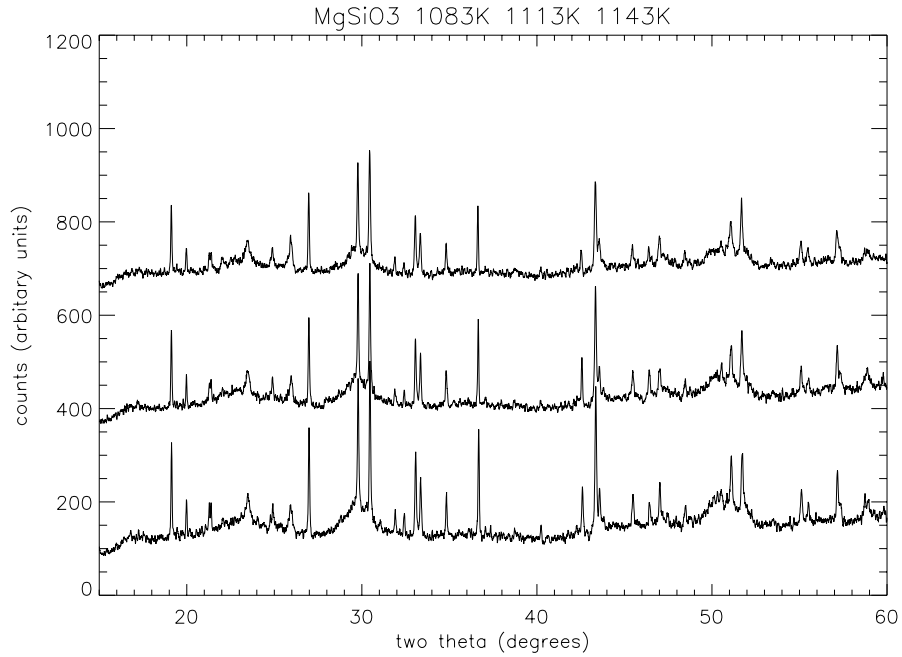

Fig. 5. $MgSiO_3$ diffraction patterns collected at (bottom to top) 1083 K, 1113 K, 1143 K, over a period of 5 hours. Note the correspondence to Figs. 3 and 4 recorded at lower temperatures

1173 K when the sample began to change. We were unable to observe any further development at 1173 K beyond 14.5 hours annealing due to limitations of beam time allocation on the synchrotron.

4. Discussion

Our results show a clear evolution of structure from a purely amorphous starting phase to a mixed amorphous/crystalline end state. Modest processing at 1000 K quickly promoted the formation of an initial crystallite along with some alteration to the remaining amorphous structure. The two phases then persisted, with little or no change, until the sample had been processed for some 79 hours and a maximum temperature reaching 1173 K, whereupon the amorphous component began to disappear and further crystal growth occurred. We propose this stall

Table 1. Measured angular peak positions and d-spaces for 1000 K and 1173 K data compared to a forsterite standard reference

1000 K crystalline structure			1173 K crystalline structure		
2θ	sample d-space (Å)	forsterite d-space (Å)	2θ	sample d-space (Å)	forsterite d-space (Å)
19.05	3.90	3.88	16.72	4.44	–
19.90	3.74	3.72	18.07	4.12	–
21.36	3.49	3.496	19.04	3.93	3.96
24.91	3.00	3.007	19.89	3.74	3.723
26.99	2.78	2.796	21.35	3.51	3.496
30.41	2.53	2.512	22.59	3.28	–
31.41	2.47	2.458	23.44	3.19	–
32.98	2.27	2.269	24.79	3.01	3.007
33.34	2.25	2.25	25.89	2.88	2.992
34.81	2.16	2.161	26.87	2.79	2.768
36.65	2.06	2.032	29.68	2.53	2.515
42.64	1.78	1.785	30.29	2.48	2.458
43.37	1.75	1.75	32.97	2.30	2.269
45.45	1.67	1.671	34.69	2.17	2.161
46.43	1.65	1.636	36.52	2.07	2.032
47.04	1.63	1.634	42.39	1.80	1.785
51.65	1.48	1.479	43.25	1.76	1.75
57.18	1.35	1.351	46.79	1.62	1.612
			51.56	1.49	1.497
			54.98	1.40	1.397

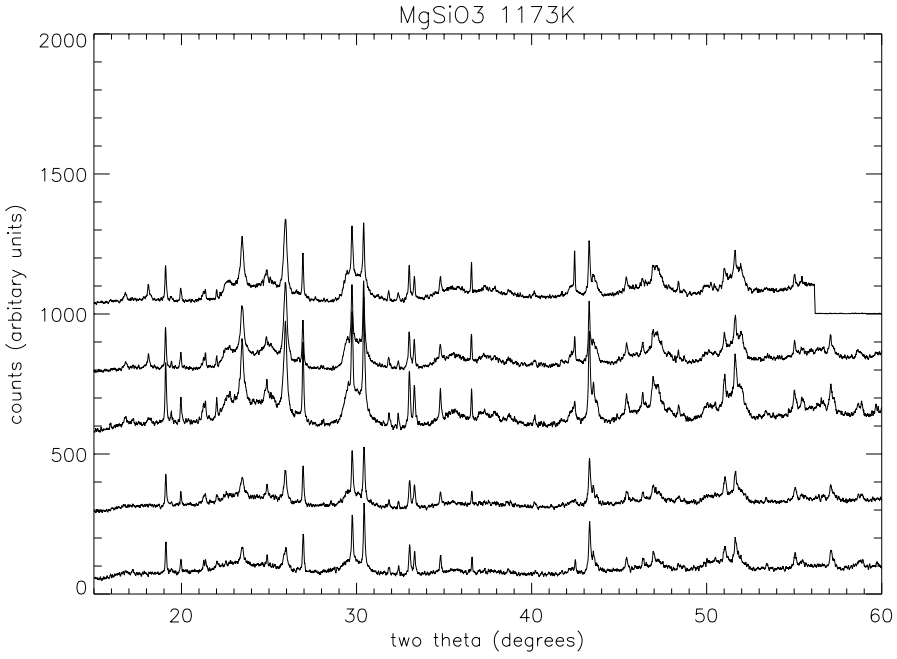

Fig. 6. $MgSiO_3$ diffraction patterns collected at 1173 K: bottom is initial exposure to this temperature, top is after 14.5 hours annealing, middle patterns are sample patterns at intermediate times. Note the changes in the top three patterns at ∼30° and ∼50° 2θ; the appearance of weak features below 19° 2θ; the development of features between 22° and 26° 2θ and the broad hump between 34° and 40° 2θ with weak features between 37° and 40° 2θ. These changes first began to manifest after ∼6 hours annealing at this temperature. The drop out at high angle in the top pattern was due to loss of the synchrotron beam

in structural development (Fig. 7) to be the likely origin of HN&D's IR spectral stall, in that their samples also initially showed pre-stall features characteristic of amorphous silicates which with annealing yielded amorphous profiles with some crystalline-like features and post-stall showed more fully developed crystalline features.

In a fixed quantity of initially amorphous material, bulk crystallisation can only proceed at the expense of the amorphous state. It is therefore the persistence of the amorphous state that inhibits crystallite development. It is well known that for an amorphous silicate there will exist a distribution of values for the number of non-bridging

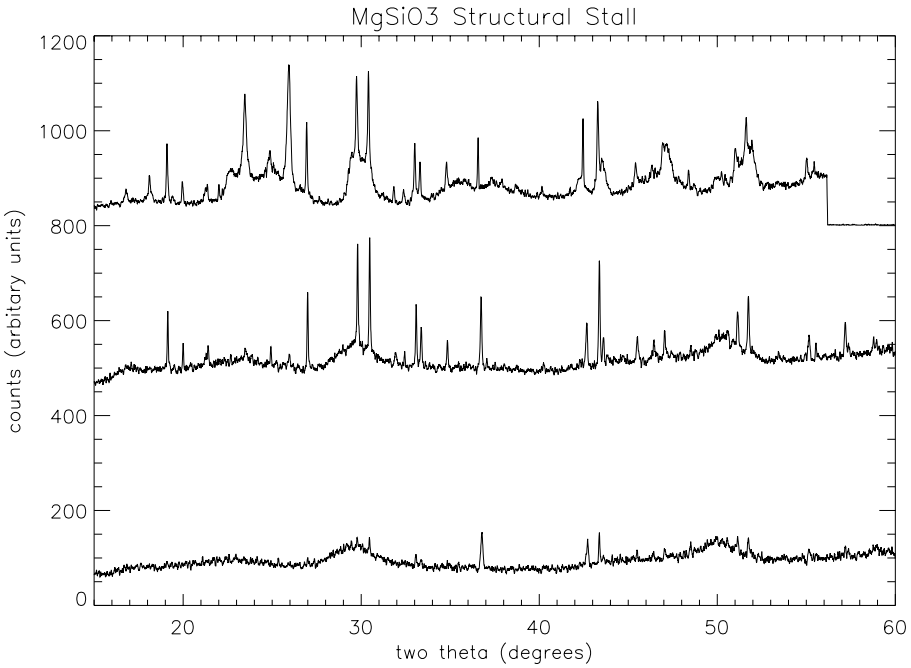

Fig. 7. Evolution of the structural stall for $MgSiO_3$: bottom, pre-stall at 1000 K as crystallite forms; middle, persistent amorphous and crystalline phases at intermediate temperatures; top, leaving the stall at 1173 K. Time difference between top and bottom data is ∼88 hours. The drop out in the top pattern is due to loss of the synchrotron beam

oxygen atoms per tetrahedral unit (NBO/T, that is O atoms that are not shared with neighbouring tetrahedra). This distribution will be peaked around the average bulk crystalline value (Farnan et al. 1992). Writing the silicate composition as $x\mathrm{MgO}(1-x)\mathrm{SiO_2}$, the average bulk crystalline NBO/T is given by (Thompson 1996)

$$NBO/T = \frac{2x}{(1-x)}. \quad (1)$$

For $MgSiO_3$ and Mg_2SiO_2, where $x = \frac{1}{2}$ and $\frac{2}{3}$ respectively, this gives bulk NBO/T values of 2 and 4. Their amorphous forms will thus contain a majority of tetrahedra with 2 and 4 NBO/T respectively, but there will also be significant numbers of other NBO/T species present. That a crystallite with the compositionally unfavourable structure Mg_2SiO_4 readily forms in an amorphous material with bulk $NBO/T = 2$, seemingly contrary to the expectations of equilibrium thermodynamics, suggests it results initially from the ordering of Mg atoms and pre-existing $NBO/T = 4$ units. In addition, X-ray absorption spectroscopy (Thompson et al. 1996) has shown the Si tetrahedral environment in amorphous silicates produced by gel desiccation to be well established. The strength of resistance to crystallisation in the amorphous phase thus largely arises from the need to break and reform multiple bonds between tetrahedral units with $NBO/T \leq 3$. Indeed, the matching of the crystalline diffraction patterns with forsterite indicates that the crystallisation process does not greatly involve tetrahedral species with $NBO/T \leq 3$, which would presumably give rise to other recognisable silicate structures visible in the diffraction patterns. If we assume the manufacturing process has resulted in an evenly distributed sample and that following annealing all available Mg contributes to the crystalline phase, removal of Mg, Si and O in the ratio of 2:1:4 from a composition of $MgSiO_3$ (1:1:3) will mean that the remaining amorphous phase will, of necessity, have a mass-balanced composition of Si and O in the ratio 1:2 (neglecting the effects of any impurities etc.) and will require an average NBO/T close to zero for that phase. Confirmation of any non-forsterite Si and O rich phase remaining amorphous is evidenced by the absence of crystalline diffraction peaks corresponding to any known form of SiO_2.

The annealing process itself may contribute to the strength of the SiO_2-rich amorphous component through dehydrogenation of the sample during annealing. Both laboratory and cosmic silicates can be expected to have significant hydroxyl content (Bruckner 1970; Steel & Duley 1987; Timmermann & Larson 1993 and references therein), while hydrogen itself can also exist in a variety of states within a silicate. Molecular hydrogen dissolves into the silicate structure over a wide range of temperatures and reacts with the silicate network to form hydroxyl (Shelby 1979; Shelby 1980), or hydroxyl/hydride pairs (van der Steen & van den Boom 1977). In the case of SiO_2, dissolved molecular hydrogen is believed to exist as lone molecules, residing in the interstices of the network (Shelby 1994). Network bonds can be broken by ionisation or direct displacement, in which case, the hydrogen present in the void spaces can react with broken bonds to form Si–OH or Si–H.

Hydroxyl and hydride are removed from amorphous SiO_2 by heating to ∼973 K or above and in the laboratory are seen to be completely removed over a period

of hours (Shelby 1994). Plotting the percentage of hydroxyl/hydride removed as a function of time, the data for each species falls on the same curve implying that the effective diffusion coefficients are the same for both species. The process of recombination yielding molecular hydrogen is (Shelby 1994),

$$\mathrm{SiOH} + \mathrm{SiH} \rightarrow \mathrm{Si–O–Si} + \mathrm{H_2}. \quad (2)$$

Measurement of the gas released during heating of other similar materials (Morimoto et al. 1992) confirms H_2 to be the major component along with very small amounts of water. Below ∼70% removal, the percentage removal curves approximate those expected for simple diffusion but yield an effective diffusion coefficient of $1.4\ 10^{-7}\ \mathrm{cm^2\,s^{-1}}$ which is much less than the expected value of $6\ 10^{-6}\ \mathrm{cm^2\,s^{-1}}$ for simple diffusion (Shelby 1977). This, taken in conjunction with observed deviations of the removal curves from that of simple diffusion above 70% removal, implies that it is the reaction rate of Eq. (2) and not the diffusion coefficient that controls the outflow of molecular hydrogen (Morimoto et al. 1992). This is supported by the activation energy of the reaction which lies between 260 $\mathrm{kJ\,mol^{-1}}$ (Heslin 1993) and 266 $\mathrm{kJ\,mol^{-1}}$ (van der Steen 1976) and which compares well with the binding energy of the SiO–H bond (264 $\mathrm{kJ\,mol^{-1}}$, Shackelford & Masaryk 1976). It is thus the breaking of this bond that controls the dehydrogenation of the silicate. Annealing an amorphous Mg-silicate at low-end (∼1000 K) temperatures is therefore likely to result in significant dehydrogenation.

The net effect of this process will be to increase the overall network polymerisation by reconnecting intertetrahedral Si-O-Si bridging bonds, which will raise the average number of bridging oxygen atoms per tetrahedral unit (i.e. decrease NBO/T). Since the silicate will initially have a distribution of NBO values, low-end annealing will initially promote the ordering of $NBO/T = 4$ species only. Crystal growth thus stalls when the need for more $NBO/T = 4$ units can only be met by breaking bonds for units with $NBO/T \leq 3$. Meanwhile, annealing induced dehydrogenation will have reduced the bulk NBO/T for these species towards that of SiO_2 (i.e. $NBO/T \rightarrow 0$). The stall thus persists until enough energy has been input to the system to allow the increased number of multiple bridging bonds to be broken, whereupon the amorphous phase breaks down and further crystal growth becomes possible.

Earlier X-ray absorption spectroscopy measurements made on the near edge structure (XANES) for the Si K shell absorption edge in these materials have shown that shifts in the position in energy of the Si K-edge XANES features are greatest for temperatures below the crystallisation threshold (Thompson et al. 1996). Such shifts are characteristic of changes in the oxidation state of the absorbing species (i.e. changes in Si polymerisation). Based on this previous evidence and our present results, it appears that the most important structural changes within the silicate occur during the annealing leading up to crystallisation. This is corroborated by HN&D's observation that the duration of the stall is longest for lower annealing temperatures.

The time scale for the formation of the initial crystallite and entry to the structural stall at 1000 K in our experiment is much shorter than that suggested by HN&D for the spectral stall (25 ± 3 days stall entry time). However, at the present time we can not rule out that this is due to differences in the starting material arising from the different methods of sample manufacture, which possibly results in different NBO/T distributions and degrees of chemical ordering. In particular, the gel desiccation method used to produce our sample will result in an evenly dispersed amorphous composition with a well established Si-O tetrahedral environment. Samples produced as smokes or ablation products on the other hand are likely to be highly disordered in both their structural and chemical ordering and will contain significant fractions of SiO, MgO and Mg-metal units. Given the limited availability of published experimental data it is not currently possible to determine the full extent to which the thermal/temporal development of either spectral or structural stall is dependent on material preparation or manufacture. From the present experiment we are also unable to address the question of whether grain size influences the crystallisation process, in particular the thermodynamic contribution of grain surface area to the eventual formation of forsterite rather than enstatite. Grain size distribution was not constrained in our experiment other than ensuring the sample powder fulfilled the requirements of the powder diffraction method to avoid settling and preferred orientation effects during the diffraction measurements.

Neither are we at present able to identify the point in the structural development of our sample where the crystalline phase will make a significant contribution to the 10 μm band profile, given that synchrotron X-ray diffraction is in general a more sensitive long range structural probe than IR spectroscopy. Experiments are currently in progress to compare diffraction with IR spectroscopy and will be reported in a subsequent paper. At the time of writing our results do however represent the only structural study in a set of three basic independent laboratory identifications of a stall phenomena in Mg-silicates (Brucato et al. 1999 have reported infrared results similar to HN&D). Each of these experiments has thus far involved samples manufactured and processed by different methods and as such our results present strong additional evidence for this being a common phenomenon in annealed Mg silicates. In that sense the production of crystalline silicates from amorphous silicates via annealing may be, to some degree, insensitive to the starting material, even though annealing profiles and other physical properties will be strongly dependent. However it is possible that this last statement may be limited in scope and that stall phenomena may in fact only occur for certain ranges of compositions and/or manufacturing parameters. Precisely what these limits are is currently unknown.

5. Conclusions

We have identified directly a structural stall in the crystalline development of thermally processed amorphous $MgSiO_3$. During the stall amorphous and crystalline phases co-exist. The development of a crystalline forsterite phase, contrary to equilibrium thermodynamic predictions, is regulated by the properties of the SiO_2-rich amorphous phase whose subsequent resistance to annealing at higher temperatures may be due to a strengthening of it's network connectivity by the annealing process itself and we have suggested a mechanism by which this can occur. Current evidence suggests this effect could be most significant when the silicate is initially annealed at low-end temperatures of ∼1000 K. Our results clearly show that an amorphous component in annealed $MgSiO_3$ can survive relatively unaltered up to temperatures higher than perhaps previously assumed. This now raises, at least in principle, the possibility of being able to extract information regarding the origins and pre-processed form of certain recovered solar system silicate grains returned by sampling missions such as STARDUST and ROSETTA, even if those grains have subsequently suffered relatively vigorous post-formation annealing. The presence of an amorphous component may prove to be of diagnostic use when attempting to differentiate non- or pre-solar components from sample populations of processed grains. The strengthening effect is likely to be most pronounced in grains that were initially exposed to lower annealing temperatures. Whether future laboratory work will enable the assignment of a unique, or limiting, thermal history to a given silicate based on some quantitative crystalline to amorphous ratio remains to be seen, however structural investigation exploiting the high angular resolution and wavelength tunability of the synchrotron source presents itself as a powerful tool with which to study cosmic silicates in the laboratory.

Acknowledgements. The authors would like to express their thanks to the anonymous referee who provided a very encouraging and constructive review of the first draft of this paper.

References

Bregman, J. D., Campins, H., Witteborn, F. C., et al. 1987, A&A, 187, 616
Brucato, J. R., Colangeli, L., Mennella, V., Palumbo, P., & Bussoletti, E. 1999, A&A, 348, 1012
Bruckner, R. 1970, J. Non-Cryst. Sol., 5, 123
Campins, H., & Ryan, B. V. 1989, ApJ, 341, 1059
Cernik, R. J., Murray, P. K., Pattison, P., & Fitch, A. N. 1990, J. Appl. Cryst., 23, 292
Collins, S. P., Cernik, R. J., Pattison, P., Bell, A. M. T., & Fitch, A. N. 1992, Rev. Sci. Instrum., 63, 1013
Crovisier, J., Brooke, T. Y., Hanner, M. S., et al. 1996, A&A, 315, L385
Day, K. L. 1974, ApJ, 234, 158
Debrenne, P., Laugier, J., & Chaudet, M. J. 1970, Appl. Cryst., 3, 493
Dorschner, J., Friedmann, C., Gurtler, J., & Henning, Th. 1988, A&A, 198, 223
Farnan, I., Grandinetti, P., Baltisberger, J. H., et al. 1992, Nature, 358, 31
Hallenbeck, S. L., & Nuth, J. A. 1998, ASS, 255, 427
Hallenbeck, S. L., Nuth, J. A., & Daukantas, P. L. 1998, Icarus, 131, 198
Hanner, M. S., Hackwell, J. A., Russell, R. W., & Lynch, D. K. 1994, Icarus, 112, 490
Hart, M., & Parrish, W. 1986, Matrls. Sci. Forum, 9, 3946
Hayward, T. L., & Hanner, M. S. 1997, Science, 275, 1907
Hecht, J. H., Russel, R. W., Stephens, J. R., & Grieve, P. R. 1986, ApJ, 309, 90
Heslin, M. R. 1993, Ph.D. Thesis, Alfred University
Hosono, H., & Abe, Y. J. 1989, J. Am. Ceram. Soc., 72, 44
Hosono, H., Abe, Y. J., & Deguchi, K. 1992, J. Non-Cryst. Sol., 142, 103
Jewell, J. M., & Aggarwal, I. D. 1995, J. Non-Cryst. Sol., 181, 189
Koike, C., & Tsuchiyama, A. 1991, in Origin and evolution of interplanetary dust, ed. A. C. Levasseur-Regourd, & H. Hasegawa (Dordrecht, KIuwer), 95
Koike, C., & Tsuchiyama, A. 1992, MNRAS, 255, 248
Morimoto, Y., Igarashi, T., Sugahara, H., & Nasu, S. 1992, J. Non-Cryst. Sol., 139, 35
Morrow, B. A., & Cody, I. A. 1973, J. Phys. Chem., 77, 1465
Munro, I. H. 1997, J. Synchrotron. Rad., 4, 344
Nuth, J. A., & Donn, B. 1982, ApJL, 257, L103
Parrish, W., Hart, M., Erickson, C. G., Masciocchi, N., & Huang, T. C. 1986, Adv. X-ray Anal., 29, 243
Russell, R. W., & Lynch, D. K. 1996, IAU Circ., 6448
Sabatier, G. 1950, C.R. Acad. Sci. Paris, 230, 1962
Shackelford, J. F., & Masaryk, J. S. 1976, J. Non-Cryst. Sol., 21, 55
Shelby, J. E. 1977, J. Appl. Phys., 48, 3387
Shelby, J. E. 1979, J. Appl. Phys., 50, 3702
Shelby, J. E. 1980, J. Appl. Phys., 51, 2589
Shelby, J. E. 1994, J. Non-cryst. Sol., 179, 138
Steel, T. M., & Duley, W. W. 1987, ApJ, 315, 337
Stephens, J. R., Blanco, A., Bussoletti, E., et al. 1995, Planet Space Sci., 43, 1241
Tang, C. C., Bushnell-Wye, C., & Cernik, R. J. 1998, J. Synchrotron. Rad., 5, 929
Tielens, A. C. G. M., Waters, L. B. F. M., Molster, F. J., & Justtanont, K. 1998, ASS, 255, 415
Thompson, S. P. 1996, Astro. Lett. Comm., 33, 299
Thompson, S. P., Evans, A., & Jones, A. 1996, A&A, 308, 309
Timmermann, R., & Larson, H. P. 1993, ApJ, 415, 820
van der Steen, G. H. A. M. 1976, Ph.D. Thesis, University of Eindhoven
van der Steen, G. H. A. M., & van den Boom, H. 1977, J. Non-Cryst. Sol., 23, 279
Walrafen, G. E. 1975, J. Chem. Phys., 62, 1373
Waters, L. B. F. M., et al. 1996, A&A, 315, L361
Wooden, D. H., Harker, D. E., Woodward, C. E., et al. 1999, ApJ, 517, 1034